Effects of ultraviolet radiation on photosynthetic performance and N_2 fixation in *Trichodesmium erythraeum* IMS 101

Xiaoni Cai[1,2], David A. Hutchins[2], Feixue Fu[2] and Kunshan Gao[1]*

[1]State Key Laboratory of Marine Environmental Science, Xiamen University, Xiamen, Fujian, 361102, China

[2]Department of Biological Sciences, University of Southern California, 3616 Trousdale Parkway, Los Angeles, California, 90089, USA

Abstract

Biological effects of ultraviolet radiation (UVR; 280–400 nm) on marine primary producers are of general concern, as oceanic carbon fixers that contribute to the marine biological CO_2 pump are being exposed to increasing UV irradiance due to global change and ozone depletion. We investigated the effects of UV-B (280-320 nm) and UV-A (320-400 nm) on the biogeochemically-critical filamentous marine N_2-fixing cyanobacterium *Trichodesmium* (strain IMS101) using a solar simulator as well as under natural solar radiation. Short exposure to UV-B, UV-A, or integrated total UVR significantly reduced the effective quantum yield of photosystem II (PSII) and photosynthetic carbon and N_2 fixation rates. Cells acclimated to low light were more sensitive to UV exposure compared to high-light grown ones, which had more UV absorbing compounds, most likely mycosporine-like amino acids (MAAs). After acclimation under natural sunlight, the specific growth rate was lower (by up to 44%), MAAs content was higher, and average trichome length was shorter (by up to 22%) in the full spectrum of solar radiation with UVR, than under a photosynthetically active radiation (PAR) alone treatment (400-700 nm). These results suggest that prior shipboard experiments in UV-opaque containers may have substantially overestimated in-situ nitrogen fixation rates by *Trichodesmium*, and that natural and anthropogenic

elevation of UV radiation intensity could significantly inhibit this vital source of new nitrogen to the current and future oligotrophic oceans.

Introduction

Global warming is inducing shoaling of the upper mixed layer and enhancing stratification, thus exposing phytoplankton cells which live in the upper mixed layer to higher depth-integrated irradiance (Häder and Gao, 2015). The increased levels of UV radiation have generated concern about their negative effects on aquatic living organisms, particularly phytoplankton, which require light for energy and biomass production.

Cyanobacteria are the largest and most widely distributed group of photosynthetic prokaryotes on the Earth, and they contribute markedly to global CO_2 and N_2 fixation (Sohm et al., 2011). Fossil evidence suggests that cyanobacteria first appeared during the Precambrian era (2.8 to 3.5 $\times 10^9$ years ago) when the atmospheric ozone shield was absent (Sinha and Häder, 2008). Cyanobacteria have thus often been presumed to have evolved under more elevated UV radiation conditions than any other photosynthetic organisms, possibly making them better equipped to handle UV radiation.

Nevertheless, a number of studies have shown that UV-B not only impairs the DNA, pigmentation and protein structures of cyanobacteria, but also several key metabolic activities, including growth, survival, buoyancy, nitrogen metabolism, CO_2 uptake, and ribulose 1,5-bisphosphate carboxylase activity (Rastogi et al., 2014). To deal with UV stress cyanobacteria have evolved a number of defense strategies, including migration to escape from UV radiation, efficient DNA repair mechanisms, programmed cell death, the production of antioxidants, and the biosynthesis of UV-absorbing compounds, such as MAAs and scytonemin (Rastogi et al., 2014; Häder et al., 2015).

The non-heterocystous cyanobacterium *Trichodesmium* plays a critical role in the marine nitrogen cycle, as it is one of the major contributors to oceanic nitrogen fixation

(Capone et al., 1997) and furthermore is an important primary producer in the tropical and sub-tropical oligotrophic oceans (Carpenter et al., 2004). This global importance of *Trichodesmium* has motivated numerous studies regarding the physiological responses of *Trichodesmium* to environmental factors, including visible light, phosphorus, iron, temperature, and CO_2 (Kranz et al., 2010; Shi et al., 2012; Fu et al., 2014; Spungin et al., 2014; Hutchins et al., 2015). However, to the best of our knowledge, nothing has been documented about how UV exposure may affect *Trichodesmium*.

Trichodesmium spp. have a cosmopolitan distribution throughout much of the oligotrophic tropical and subtropical oceans, where there is a high penetration of solar UV-A and UV-B radiation (Carpenter et al., 2004). It also frequently forms extensive surface blooms (Westberry and Siege, 2006), where it is presumably exposed to very high levels of UV radiation. Moreover, in the ocean, *Trichodesmium* populations may experience continuously changing irradiance intensities as a result of vertical mixing. Cells photoacclimated to reduced irradiance at lower depths might be subject to solar UVR damage when they are vertically delivered close to the sea surface due to mixing. Therefore, this unique cyanobacterium may have developed defensive mechanisms to overcome harmful effects of frequent exposures to intense UV radiation. Understanding how its N_2 fixation and photosynthesis respond to UV irradiance will thus further our knowledge of its ecological and biogeochemical roles in the ocean.

When estimating N_2 fixation using incubation experiments in the field, marine scientists have typically excluded UV radiation by using incubation bottles made of UV-opaque materials like polycarbonate (Capone et al., 1998; Olson et al., 2015). Thus, it seems possible that most shipboard measurements of *Trichodesmium* N_2 fixation rates could be overestimates of actual rates under natural UV exposure conditions in the surface ocean. In this study, *Trichodesmium* was exposed to spectrally realistic irradiances of UVR in laboratory experiments to examine the short-term effects of UVR on photosynthesis and N_2 fixation. In addition, *Trichodesmium* was grown under natural solar irradiance outdoors in order to assess UV impacts on longer timescales, and to test

for induction of protective mechanisms to ameliorate chronic UV exposure effects.

Materials and methods

Study strategy This study included two parts: (1) A short-term experiment under a solar stimulator (refer to Fig.S1 for the spectrum) to examine the responses of *Trichodesmium erythraeum* IMS 101 to a range of acute UV radiation exposures, and (2) A long-term UV experiment under natural sunlight to examine acclimated growth and physiology of *Trichodesmium* IMS 101. The first set of experiments was intended to mimic intense but transitory UV exposures, as might occur sporadically during vertical mixing, while the second set was intended to give insights into responses during extended near-surface UV exposures, such as during a surface bloom event.

Short-term UV experiment *Trichodesmium erythraeum* IMS101 strain was isolated from the North Atlantic Ocean (Prufert-Bebout et al., 1993) and maintained in laboratory stock cultures in exponential growth phase in autoclaved artificial seawater enrich with nitrogen free YBCII medium (Chen et al., 1996). For the short-term UV experiment, the cells were grown under low light (LL) 70 μmol photons m^{-2} s^{-1} and hight light (HL) 400 μmol photons m^{-2} s^{-1} (12:12 light: dark) of PAR for at least 50 generations (about 180 days) prior to the UV experiments. These two light levels represent growth sub-saturating and super-saturating levels for *Trichodesmium* (Cai et al., 2015). Cultures were grown in triplicate using a dilute semi-continuous culture method, with medium renewed every 4-5 days at 25ºC. The cell concentration was maintained at $< 5 \times 10^4$ cell ml^{-1}.

To determine the short-term responses of *Trichodesmium* IMS101 to UV radiation, subcultures of *Trichodesmium* IMS101 were dispensed at a final cell density of 2-4 × 10^4 cells ml^{-1} into containers that allow transmission of all or part of the UV spectrum, including 35 ml quartz tubes (for measurements of carbon fixation or measurements of fluorescence parameters), 100 ml quartz tubes (for pigment measurements), or 13 ml

gas-tight borosilicate glass vials (for N_2 fixation measurements). Three triplicated radiation treatments were implemented: (1) PAB (PAR+UV-A+UV-B) treatment, using tubes covered with Ultraphan film 295 (Digefra, Munich, Germany), thus receiving irradiances >295 nm; (2) PA (PAR+UV-A) treatment, using tubes covered with Folex 320 film (Montagefolie, Folex, Dreieich, Germany), and receiving irradiances >320 nm; and (3) P treatment: tubes covered with Ultraphan film 395 (UV Opak, Digefra), with samples receiving irradiances above 395 nm, representing PAR (400-700 nm). Since the transmission spectrum of the borosilicate glass was similar to that of Ultraphan film 295, the borosilicate glass vials for N_2 fixation measurements of PAB treatment were uncovered. Transmission spectra of these tubes (quartz and borosilicate) and the various cut-off foils used in this study are shown in Fig. S1.

The experimental tubes were placed under a solar simulator (Sol 1200W; Dr. Hönle, Martinsried, Germany) at a distance of 110 cm from the lamp, and maintained in a circulating water bath for temperature control (25°C) (CTP-3000, Eyela, Japan). Irradiance intensities were measured with a LI-COR 2π PAR sensor (PMA2100, Solar light, USA) that has channels for PAR (400-700 nm), UV-A (320-400 nm) and UV-B (280-320 nm). Measured values at the 110 cm distance were 87 Wm^{-2} (PAR, ca. 400 μmol photons m^{-2} s^{-1}), 28 Wm^{-2} (UV-A) and 1 Wm^{-2} (UV-B), respectively. For the fluorescence measurements, samples were exposed under a solar stimulator for 60 min and measurements of fluorescence parameters were performed during the exposure (see below). Due to analytical sensitivity issues, for the carbon and N_2 incorporation measurements, the exposure duration was 2 hrs, and for the measurements of UVAC (UV-absorbing compounds) contents, the exposure time was 10 hrs.

Long-term UV experiment To assess the long-term effects of solar ultraviolet radiation on *Trichodesmium* IMS101, an outdoor experiment was carried during the winter (Jan 1st to Jan 26th, 2014) in subtropical Xiamen, China. 300-400 ml cell cultures were grown in 500 ml quartz vessels exposed to 100% daytime natural solar irradiance (surface ocean irradiance) (daytime PAR average of ~120W m^{-2}, highest PAR at noon

~300W m^{-2}). All of the quartz vessels were placed in a shallow water bath at 25°C using a temperature control system (CTP-3000, Eyela, Japan). Two triplicated radiation treatments were implemented: (1) treatment P: PAR alone (400-700 nm), tubes covered with Ultraphan film 395 (UV Opak, Digefra); (2) treatment PAB: PAR+UV-A+UV-B (295-700 nm), unwrapped quartz tubes. Incident solar radiation was continuously monitored with a broadband Eldonet filter radiometer (Eldonet XP, Real Time Computer, Möhrendorf, Germany) that was placed near the water bath. Daily doses of solar PAR, UV-A and UV-B during the experiments are shown in Fig. S2. The photoperiod during the outdoor incubation was 11:13 light:dark (light period from 7:00-18:00 of local time). Cells were maintained in exponential growth phase (cell density < 5×10^4), with dilutions (after sunset) every 4 days. All parameters were measured after acclimation under P or PAB radiation for a week.

Specific growth rate (μ, d^{-1}) of *Trichodesmium* IMS101 was determined based on the change in cell concentrations over 4 days during the 8-11th and 12-15th day using microscopic counts (Cai et al., 2015), the corresponding total dose from Day 8 to Day 11 and from Day 12 to Day 15 were 17.03 and 18.51 MJ m^{-2}, respectively. Chl *a* content was measured at the 11th, 15th and 19th day, and Chl *a*-specific absorption spectrum was measured at the 18th day. Carbon and N_2 fixation rate were measured at 11:00-13:00 on the 18th day; the diel solar irradiance record on that day is given in Fig. S3. In order to separate the respective effects of UV-A and UV-B on carbon and N_2 fixation, a shift experiment was carried out: subcultures from either P or PAB treatments were transferred into another P (PAR), PA (PAR+UV-A), PAB (PAR+UV-A+UV-B) treatment, which were marked as P′, PA′, PAB′ treatments, respectively (namely P grown cells divided into P′, PA′, PAB′ treatments; PAB grown cells also divided into P′, PA′, PAB′ treatments). 35 ml quartz tubes and 13 ml gas-tight borosilicate glass vials were used for carbon and N_2 fixation measurements, respectively, as described below. Triplicate samples were used for each radiation treatment for carbon and N_2 fixation, and the incubations were performed under 100% solar irradiance for 2 hrs.

Measurements and analyses

Effective photochemical quantum yield During the exposure under the solar stimulator in the short-term experiment, small aliquots of cultures (2 ml) were withdrawn at time intervals of 3-10 min and immediately measured (without any dark adaptation) using a Pulse-Amplitude-Modulated (PAM) fluorometer (Xe-PAM, Walz, Germany). The quantum yield of PSII (F_V'/F_M') was determined by measuring the instant maximum fluorescence (F_M') and the steady state fluorescence (Ft) under the actinic light. The maximum fluorescence (F_M') was determined using a saturating light pulse (4000 μmol photons m^{-2} s^{-1} in 0.8 s) with the actinic light level set at 400 μmol photons m^{-2} s^{-1}, similar to the PAR level during the solar simulator exposure The quantum yield was calculated as: $F_V'/F_M' = (F_M'-Ft)/F_M'$ (Genty et al., 1989).

Chlorophyll-specific absorption spectra and UV-absorbing compounds (UVACs) Chl *a*-specific absorption spectra were measured on the 18th day, after consecutive sunny days. Cellular absorption spectra were measured using the ‘‘quantitative filter technique’’ (Kiefer and SooHoo, 1982; Mitchell 1990). The cells were filtered onto GF/F glass fiber filters and scanned from 300 to 800 nm using a 1-nm slit in a spectrophotometer equipped with an integrating sphere to collect all the transmitted or forward-scattered light (i.e., light diffused by the filter and the quartz diffusing plate). Filters soaked in culture medium were used as blanks. Chlorophyll-specific absorption cross-sections (a*) were calculated according to Cleveland and Weidemann (1993) and Anning et al., (2000). Content of Chl *a* and UV-absorbing compounds (UVACs) were measured by filtering the samples onto GF/F filters and subsequently extracted in 4 mL of 100% methanol overnight in darkness at 4 ^{o}C. The absorption of the supernatant was measured by a scanning spectrophotometer (Beckman Coulter Inc., Fullerton, CA, USA). The concentration of Chl *a* was calculated according to Ritchie (2006). The main absorption values for UV-absorbing compounds ranged between wavelengths of 310 and 360 nm, and the peak absorption value at 332 nm was used to estimate total absorptivity of UVACs according to Dunlap et al., (1995). The absorptivity of UVACs

was finally normalized to the Chl *a* content (μg (μg Chl *a*)$^{-1}$).

Trichodesmium IMS101 UVACs content was compared to that of three other marine phytoplankton species, including *Chlorella*.sp, *Phaeodactylum tricornutum*, and *Synechococcus* WH7803, representing a green alga, a diatom and a unicellular cyanobacterium, respectively. All cultures were maintained under the same conditions (25ºC, 150 μmol photons m^{-2} s^{-1}) for several days prior to pigment extraction. The absorption spectra were measured by filtering the samples on GF/F filters that were subsequently extracted in 4 mL of 100% methanol overnight at 4 ºC. The absorption spectra of the supernatant were scanned from 250 to 800 nm in a spectrophotometer (Beckman Coulter Inc., Fullerton, CA, USA). The Optical Density (OD) values were then normalized to OD (662 nm), Chl *a* peak.

Carbon fixation rates Carbon fixation rate of both short- and long-term experiments were measured using the ^{14}C method. A total of 20 ml samples were placed in 35 ml quartz tubes and inoculated with 5μCi (0.185 MBq) of labeled sodium bicarbonate (ICN Radiochemicals), and were then maintained under the corresponding radiation treatments for 2 hrs. After incubation, the cells were filtered onto Whatman GF/F filters (Φ 25 mm) and stored at -20ºC until analysis. To determine the radioactivity, the filters were thawed and then exposed to HCl fumes overnight and dried at 60ºC for 4 hrs before being placed in scintillation cocktail (Hisafe 3, Perkin-Elmer, Shelton, CT, USA), and measured with a scintillation counter (Tri-Carb 2800TR, Perkin-Elmer, Shelton, CT, USA) as previously described (Cai et al., 2015).

N_2 fixation rates Rates of N_2 fixation for both short- and long-term experiments were measured in parallel with the carbon fixation measurements using the acetylene reduction assay (ARA) (Capone et al., 1993). Samples of 5 ml subcultures were placed in 13 ml gas-tight borosilicate vials (described above), and 1ml acetylene was injected into the headspace before incubating for 2 hrs under the corresponding radiation treatment conditions. A 500 μl headspace sample was then analyzed in a gas

chromatograph equipped with a flame-ionization detector and quantified relative to an ethylene standard. The ethylene produced was calculated using the Bunsen gas solubility coefficients according to Breitbarth et al., (2004) and an ethylene production to N_2 fixation conversion factor of 4 was used to derive N_2 fixation rates, which were then normalized to cell number.

Data analysis The inhibition of ΦPSII, carbon fixation and N_2 fixation due to UVR, UV-A, or UV-B was calculated as:

$$\text{UVR-induced inhibition} = (I_P - I_{PAB})/I_P \times 100\%$$

$$\text{UV-A-induced inhibition} = (I_P - I_{PA})/I_P \times 100\%$$

$$\text{UV-B-induced inhibition} = UVR_{inh} - UVA_{inh}$$

where I_P, I_{PA}, I_{PAB} indicate the values of carbon fixation or N_2 fixation in the P, PA and PAB treatments, respectively. Repair (r) and damage (k) rates during the 60 min exposure period in the presence of UV were calculated using the Kok model (Heraud and Beardall, 2000):

$$P/P_{initial} = r/(r+k) + k/(r+k) \times \exp(-(r+k) \times t),$$

where $P_{initial}$ and P were the yield values at the beginning and at exposure time t. Three replicates for culture conditions or each radiation condition was used in all experiments, and the data are plotted as mean and standard deviation values. Two way ANOVA tests were used to determine the interaction between culture conditions and UVR at a significance level of $p=0.05$.

Results

Short-term UV experiment The effects of acute UVR exposure on cells grown under LL and HL conditions are shown in Fig.1. For the cells grown under LL condition, the F_V'/F_M' declined sharply within 10 min after first exposure in all radiation treatments,

and then leveled off. F_V'/F_M' decreased less in the samples receiving PAR alone (to 43% of the initial value) than those additionally receiving UV-A (to 30% of the initial value) or UV-A+UV-B (to 24% of the initial value) (Fig.1A). The F_V'/F_M' value of PA and PAB treatments were significantly lower compared to the PAR treatment ($p=0.03$ and $p<0.01$, respectively). F_V'/F_M' of HL grown cells declined less and more slowly compared to the LL grown cells. The F_V'/F_M' of HL cells under PAR alone remained more or less constant during the exposure, since the PAR level was similar to the growth level of HL (400 μmol photons m^{-2} s^{-1}). In contrast, the F_V'/F_M' decreased to 75% and 65% of its initial value for the PA and PAB treatment, respectively, and were significantly lower than the PAR treatment ($p<0.01$) (Fig.1B).

The damage and repair rates of the PSII reaction center estimated from the exponential decay in the effective quantum yield showed higher damage and lower repair rates in the LL-grown cells than in the HL-grown ones (Fig.1C,D). The PSII damage rates (k, min^{-1}) of LL grown cells were 0.14, 0.16 and 0.15 min^{-1} in the P, PA and PAB treatments, respectively, about 2 times faster than in the cells grown under HL conditions (Fig.1C). The PSII repair rates (r, min^{-1}) of LL grown cells were 0.1, 0.06 and 0.05 min^{-1} in the P, PA and PAB treatments, which were 83% ($p<0.01$), 33% ($p<0.01$) and 54% ($p<0.01$) lower than in HL grown cells, respectively (Fig.1D). The damage rate was not significantly different among P, PA and PAB treatments within either of the LL- and HL-grown treatments ($p>0.05$), but the repair rate was much higher in the P treatment without UV than in PA or PAB treatments in the HL-grown cells ($p<0.01$).

The photosynthetic carbon fixation and N_2 fixation rates during the UV exposure are shown in Fig. 2. The HL-grown cells had 17% higher photosynthetic carbon fixation rates than the LL-grown ones under the PA treatment ($p<0.01$), however, the LL and HL-grown cells didn't show significant differences in carbon fixation rates under the P and PAB treatments ($p=0.29$, and $p=0.06$). In the presence of UV radiation, carbon fixation was significantly inhibited in both LL and HL-grown cells (Fig.2A). Carbon fixation inhibition induced by UV-A was about 35-45%, much larger than that induced

by UV-B, which caused only about a 10% inhibition of carbon fixation ($p<0.01$). The UV-A exposed carbon fixation rate was significantly higher in the LL- grown cells than in HL grown cells ($p<0.01$), while UV-B did not cause a significant difference in inhibition between the HC- and LC-grown cells ($p=0.88$) (Fig. 2B). N_2 fixation rates were about twofold higher in HL-grown cells in all radiation treatments (Fig.2C, $p<0.01$), but the UV-induced N_2 fixation inhibition showed no significant differences between the LL and HL grown cells regardless of UV-A or UV-B exposures (Fig. 2D, $p=0.80$, 0.62, 0.39 for UVA-, UVB-, and UVR-induced inhibition, respectively).

Compared to other phytoplankton under the same growth conditions, *Trichodesmium* IMS101 had much higher absorbance in the UV region (300-400 nm) (Fig. 3A). In this study, the absorbance at 332 nm of HL-grown cells was about twofold higher compared to LL-grown ones (Fig. 3B). However, the cellular Chl *a* content (data not shown) and UVACs contents of both LL and HL grown cells did not change after exposure to UV for 10 hrs (Fig. 3C).

Long-term UV experiment After being acclimated under full natural solar radiation for 7 days, the specific growth rates of cells grown under the PAB treatment were 0.15 ± 0.01 and 0.14 ± 0.06 during the 8-11th day and 12-15th day periods, respectively. These growth rates were significantly lower by 44% and 39% compared to cells grown under the P treatment, respectively (Fig.4A, $p=0.014$ and $p=0.03$). The mean trichome lengths of PAR treatment cells on the 11th and 15th day were 758 ± 56 and 726 ± 19 μm, while addition of UVR significantly reduced the trichome length by 22% (Day 11th, $p=0.02$)and 11% (Day 15th, $p=0.02$).

Analysis of the Chl *a* specific absorption spectra, $a^*(\lambda)$, demonstrated that UVR had a major effect on the absorbance of UV regions and phycobilisomes (Fig. 5). The optical absorption spectra revealed a series of peaks in the UV and visible wavelengths corresponding to the absorption peaks of UVACs at 332 nm, Chl *a* at 437 and 664 nm, phycourobilin (PUB) at 495 nm, phycoerythrobilin (PEB) at 545 nm,

phycoerythrocyanin (PEC) at 569 nm, and phycocyanin (PC) at 627 nm. In the UV region, the a*(λ) value was higher in the PAB treatment cultures than in the P treatment cultures (Fig. 5). The UVR treatments did not show clear effects on Chl *a* content compared to acclimation to PAR alone measured on different days (Fig. S3). However, the ratio of UVACs to Chl *a* was increased by 41% in the PAB compared to the P treatment ($p<0.01$).

The cells grown in the long-term P and PAB treatments showed different responses for carbon and N_2 fixation after being transferred to short-term P′, PA′, and PAB′ radiation treatments at noon on the 18th day (Fig. 6). P and PAB acclimated cells did not show significant differences in carbon fixation among all short-term P′, PA′, PAB′ treatments (Fig. 6A, $p=0.17$, $p=0.22$, $p=0.51$, respectively), nor in the UV-induced inhibition of carbon fixation (Fig. 6B, $p>0.05$). However, long-term UV-A exposure inhibited short-term carbon fixation by about 58% in both the P and the PAB treatments, significantly higher than that induced by UV-B radiation (Fig. 6B, $p<0.01$).

N_2 fixation rates of P acclimated cells were significantly higher than PAB acclimated cells in all P′, PA′, and PAB′ treatments (Fig. 6C, $p<0.01$). The N_2 fixation inhibition induced by UV-A of PAB acclimated cells was 49%, significantly higher by 47% than that of P acclimated cells ($p=0.03$), while there was no significant difference in UVB-induced N_2 fixation inhibition between P and PAB acclimated cells (Fig. 6D, $p=0.62$). The carbon fixation rates measured under PAR (PAR treated cells to P') and PAB (PAB treated cells to PAB') conditions were 89.2 and 47.1 fmol C cell^{-1} h^{-1}, respectively, while N_2 fixation rates measured under those conditions were 1.9 and 0.5 fmol N_2 cell^{-1} h^{-1}. UVR exposure lowered estimates of carbon and N_2 fixation rates by 47% and 65%, respectively.

Discussion

Our study shows that growth, photochemistry, photosynthesis and N_2 fixation in

Trichodesmium.sp are all significantly inhibited by UVR, including both UV-A and UV-B. These effects occur in both short-term, acute exposures, as well as after extended exposures during acclimated growth. These results are ecologically relevant, since this cyanobacterium is routinely exposed to elevated solar irradiances in its tropical habitat either transiently, during vertical mixing, or over longer periods during surface blooms. *Trichodesmium* provides a biogeochemically-critical source of new N to open ocean food webs, so significant UV inhibition of its growth and N_2 fixation rates could have major consequences for ocean biology and carbon cycling.

Short exposure to UVR causes a significant decline in the quantum yield of photosystem II (PSII) fluorescence of *Trichodesmium*, that is consistent with damage to critical PSII proteins such as D1 in a brackish water cyanobacterium *Arthrospira (Spirulina) platensis* (Wu et al., 2011). UV-induced degradation of D1 proteins results in inactivation of PSII, leading to reduction in photosynthetic activity (Campbell et al., 1998). In addition, studies of various microbial mats have shown that Rubisco activity and supply of ATP and NADPH are inhibited under UV exposure, which might also lead to the reduction in photosynthetic carbon fixation (Cockell and Rothschild, 1999; Sinha et al., 1996, 1997).

Exposure to UVR had an impact on nitrogenase activity in *Trichodesmium*, since both the short- and the long-term UV exposure led to significant reduction of N_2 fixation of up to 30% (short-term) or ~60% (long-term) (Fig. 2D and 6D). Studies on the freshwater cyanobacterium *Anabaena*. sp. showed a 57% decline in N_2 fixation rate after 30min exposure to UVR of 3.65W (Lesser, 2007). Some rice-field cyanobacteria completely lost N_2 fixation activity after 25-40 min exposure to UV-B of 2.5 W (Kumar et al., 2003). In our results, long-term exposure to UV led to higher inhibition of N_2 fixation, implying that accumulated damage to the key N_2-fixing enzyme, nitrogenase, could have occurred during the growth period under solar radiation in the presence of UVR.

Compared to N_2 fixation, UVR induced an even higher degree of inhibition of carbon fixation. The carbon fixation rate decreased by 50% in the presence of UVR. UV-A induced higher inhibition than UV-B, indicating that although UV-B photons (295-320 nm) are in general more energetic and damaging than UV-A (320-400 nm), the greater fluxes of UV-A caused more inhibition of carbon fixation, which was consistent with other studies of spectral dependence of UV effects (Cullen and Neale 1994; Neale 2000). This finding is ecologically significant, since UV-A penetrates much deeper into clear open ocean and coastal seawater than does UV-B.

Compared to low light-grown cells, the high light-grown ones were more resistant to UVR, which was reflected in the lower PSII damage rate and faster recovery rate in the presence of UVR, as well as the significantly lower levels of carbon fixation inhibition caused by UV-A and/or UV-B. Such a reduced sensitivity to UVR coincided well with a significant increase in UV-absorbing compounds in the HL-grown cells compared to the LL-grown ones. Similar dependence of photosynthetic sensitivity to UV inhibition on growth light levels has been reported in other species of phytoplankton (Litchman and Neale, 2005; Sobrino and Neale, 2007). A red-tide dinoflagellate *Gymnodinium sanguineum Hirasaka* accumulates 14-fold MAAs in high-light grown cells (76 W m^{-2}) than in low-light grown ones (15 W m^{-2}) and the former ones have lower sensitivity to UV radiation at wavelengths strongly absorbed by the MAAs (Neale et al., 1998). The sensitivity of PSII quantum yield to UV exposure in *Synechococcus* WH7803 was also less in high-light-grown versus low-light-grown cells (Garczarek et al., 2008). In addition, it has been observed that phytoplankton from turbid waters or acclimated to low-light conditions are more sensitive to UVR than those from clear waters (Villafane et al., 2004; Litchman and Neale, 2005; Helbing et al., 2015). These observations suggest that *Trichodesmium* sp. may acclimate to growth in the upper mixed layer by producing UV-absorbing compounds, making them more tolerant of UVR than cells living at deeper depths.

Although UV radiation can clearly cause damage to PSII and inhibit physiological

processes in *Trichodesmium* sp., this cyanobacterium has evolved protective biochemical mechanisms to deal with UV radiation in their natural high-UV habitat. One important class of UV-absorbing substances are mycosporine-like amino acids (MAAs) and scytonemin. These compounds strongly absorb in the UV-A and/or UV-B region of the spectrum, and dissipate its energy as heat without forming reactive oxygen species, protecting the cells from UV and from photooxidative stress (Banaszak 2003). The ‘‘mycosporine-like amino acids’’ (MAAs), which have strong UV-absorption maxima between 310 and 362 nm (Sinha and Häder, 2008) as identified by HPLC in other studies, consist of a group of small, water-soluble compounds, including asterina-332 (λmax=332) and shinorine (λmax=334), which are the most abundant, as well as mycosporine-glycine (λmax=310), porphyra-334 (λmax=334), and palythene (λmax=360) (Shick and Dunlap 2002; Subramaniam et al., 1999). As was found previously in *Trichodesmium* spp., high absorbance in the UV region is mainly due to the presence of ‘‘mycosporinelike amino acids’’ (MAAs), with absorbance maxima between 310~362 nm (Sinha and Häder, 2008).

Our investigation strongly suggests that *Trichodesmium* is able to synthesize MAAs (λmax ~330 nm and 360 nm) in response to elevated PAR and UV radiation. Synthesis of MAAs has been reported to be stimulated by high PAR and UV radiation in other phytoplankton (Karsten et al., 1998; Vernet and Whitehead, 1996; Sinha et al., 2001). Our high light-grown cells were more tolerant of UVR, likely at least partly due to their ability to synthesize double the amount of MAAs in comparison to low light-grown ones (Fig.3B). It has been showed that accumulation of MAAs may represent a natural defensive system against exposure to biologically harmful UV radiation (Karsten et al., 1998) and cells with high concentrations of MAAs are more resistant to UVR than cells with small amounts of these compounds (Garcia-Pichel and Castenholz, 1993). In fact, MAAs concentrations varying between 0.9 and 8.4 ug mg (dry weight)$^{-1}$ have been measured in cyanobacterial isolates (Garcia-Pichel and Castenholz, 1993), and ratios of MAAs to Chl *a* in the range from 0.04 to 0.19 have been reported in

cyanobacterial mats (Quesada et al., 1999). In our study, we found that *Trichodesmium* contained a much higher concentration of MAAs (the highest value in HL-grown cells is 5 pg cell^{-1}) and that the ratio of these compounds to Chl *a* was 5, was consisted with previous reports in regard to *Trichodesmium* (Subramaniam et al., 1999), which is much higher than in other phytoplankton. This adaptation could be a major reason for the ability of *Trichodemium* to grow and form extensive surface blooms under strong irradiation in the oligotrophic oceans.

In our study, no significant changes in the amount of MAAs were observed after 10 h of exposure to UVR under the solar simulator. In contrast, a significant increase of 23% in the concentration of MAAs was observed in full solar spectrum treated cells compared to PAR-treated ones grown outdoors after consecutive sunny days (on the 18th). It seems that the synthesis of MAAs takes a relatively long time. Other studies have shown the time required for induction of MAAs in other cyanobacteria is dependent on UV doses and species, and shows a circadian rhythm (Sinha et al., 2001; Sinha et al., 2003).

Not only did long-term exposure to high solar UV radiation significantly reduce *Trichodesmium*'s growth rate (by 37~44%), but it also significantly shortened its average trichome length (less cell per filament) (Fig. 4). The decreased growth rates correlated with decreased trichome length are consistent with our previous studies under different light levels without UVR (Cai et al., 2015). It has been reported that enhanced UVR is one of the environmental factors that not only inhibit the growth of cyanobacteria, but also change their morphology (Rastogi et al., 2014). Natural solar UVR can suppress formation of heterocysts and shorten the filament length of *Anabaena* sp. PCC7120 (Gao et al., 2007). Natural levels of solar UVR in the Southern China were also found to break the filaments and alter the spiral structure of *Arthrospira* (*Spirulina*) *platensis*, with a compressed helix that lessens UV exposures for the cells (Wu et al., 2005). Cells in the trichomes of the estuarine cyanobacterium *Lyngbya aestuarii* coil and then form small bundles in response to UV-B irradiation (Rath and

Adhikari, 2007). However, the shortened trichomes of *Trichodesmium* in this work may be a result of UV-inhibited growth rather than a responsive strategy against UV.

Carbon fixation in the long-term experiment showed similar patterns with the short-term UV experiment, demonstrating that UV-A played a larger role in inhibiting carbon fixation than UV-B. Since the ratio of UV-B to UV-A is lower in natural solar light (1:50) than under our artificial UVR (1:28), the inhibitory effects of UV-B were smaller compared to UV-A in the cultures under sunlight. Carbon fixation and N_2 fixation rates measured outdoors indicated that UV-induced carbon fixation inhibition recovers quickly following transfer to PAR conditions, while the UV-induced N_2 fixation inhibition does not (Fig.6AC). Factors that might be responsible include lower turnover rate of nitrogenase than that of RuBisco; more UV-induced damage to nitrogenase with lower efficiency of repair (Kumar et al., 2003); and indirect harm caused by ROS (Reactive Oxygen Species) induced by UV (Singh et al., 2014).

The UV effects in our study were measured under conditions that minimized self-shading, namely during growth as single filaments. However, in its natural habitat *Trichodesmium* often grows in a colonial form, with packages of many cells held together by an extracellular sheath (Capone et al., 1998). In such colonial growth forms, the effective cellular pathlengths for UV radiation are likely greatly increased, thereby amplifying the overall sunscreen factor for the colony. *Trichodesmium*.spp might use this colony strategy to protect themselves from natural UV damage in the ocean.

Our investigation shows that this cyanobacterium appears to have evolved the ability to produce exceptionally high levels of UV protective compounds, likely mycosporine-like amino acids. However, even this protective mechanism is insufficient to prevent substantial inhibition of nitrogen and carbon fixation in the high-irradiance environment where this genus lives. *Trichodesmium* spp are distributed in the upper layers of the euphotic zone in oligotrophic waters, and its population densities are generally greatest at relatively shallow depths (20 to 40 m) in the upper water column

(Capone et al., 1997). It seems likely that UV inhibition therefore significantly reduces the amount of critical new nitrogen supplied by *Trichodesmium* to the N-limited oligotrophic gyre ecosystems, a possibility that has not been generally considered in regional or global models of the marine nitrogen cycle. On the other hand, the UV absorbing compounds (most likely MAAs) are expensive to make in terms of nitrogen in particular (Singh et al., 2008). Decreased nitrogen supplied may increase sensitivity of phytoplankton assemblages to UV further (Litchman et al 2002), thus potentially creating a positive feedback between N-limitation and the UV sensitivity.

Trichodesmium can form dense, extensive blooms in the surface oceans, and a frequently cited estimate of global nitrogen fixation rates by *Trichodesmium* blooms is ~42 Tg N yr^{-1} (Westberry et al., 2006). Previous biogeochemical models of global N_2 fixation have emphasized controls by many environmental factors, including solar PAR radiation, temperature, wind speed, and nutrient concentrations (Luo et al., 2014), but have largely neglected the effects of UV radiation. When estimating N_2 fixation using incubation experiments in the field, however, marine scientists have typically excluded UV radiation by using incubation bottles made of UV-opaque materials like polycarbonate (Olson et al., 2015). Our results suggest that under solar radiation at the surface ocean, including realistic levels of UVR inhibition lowers estimates of carbon fixation and N_2 fixation by around 47% and 65%, respectively (Fig.6).

Thus, it seems likely that shipboard measurements and possibly current model projections of *Trichodesmium* N_2 fixation and primary production rates that do not take into account UV inhibition could be substantial overestimates. However, our study was only carried out under full solar radiation, simulating sea surface conditions, so further studies are needed to investigate depth-integrated UV inhibition. Moreover, the response to UV radiation may be taxon-specific. For example, unicellular N_2-fixing cyanobacteria such as the genus *Crocosphaera*, with smaller cell size and thus greater light permeability, may be more vulnerable to UV radiation than *Trichodesmium* (Wu et al., 2015). In the future, as enhanced stratification and decreasing mixed layer depth

expose cells to relatively higher UV levels, differential sensitivities to UV radiation may result in changes in diazotroph community composition. Such UV-mediated assemblage shifts could have potentially major consequences for marine productivity, and for the global biogeochemical cycles of nitrogen and carbon.

Acknowledgements

This study was supported by the National Key Research Programs 2016YFA0601400 and National Natural Science Foundation (41430967; 41120164007) to KSG, and by U.S. National Science Foundation grants OCE 1260490 and OCE 1538525 to F-X.F. and D.A.H. DAH and F-X.F.'s visit to Xiamen was supported by MEL's visiting scientists programs. The authors would like to thank Nana Liu and Xiangqi Yi from Xiamen University for their kind assistance during the experiments.

Figures

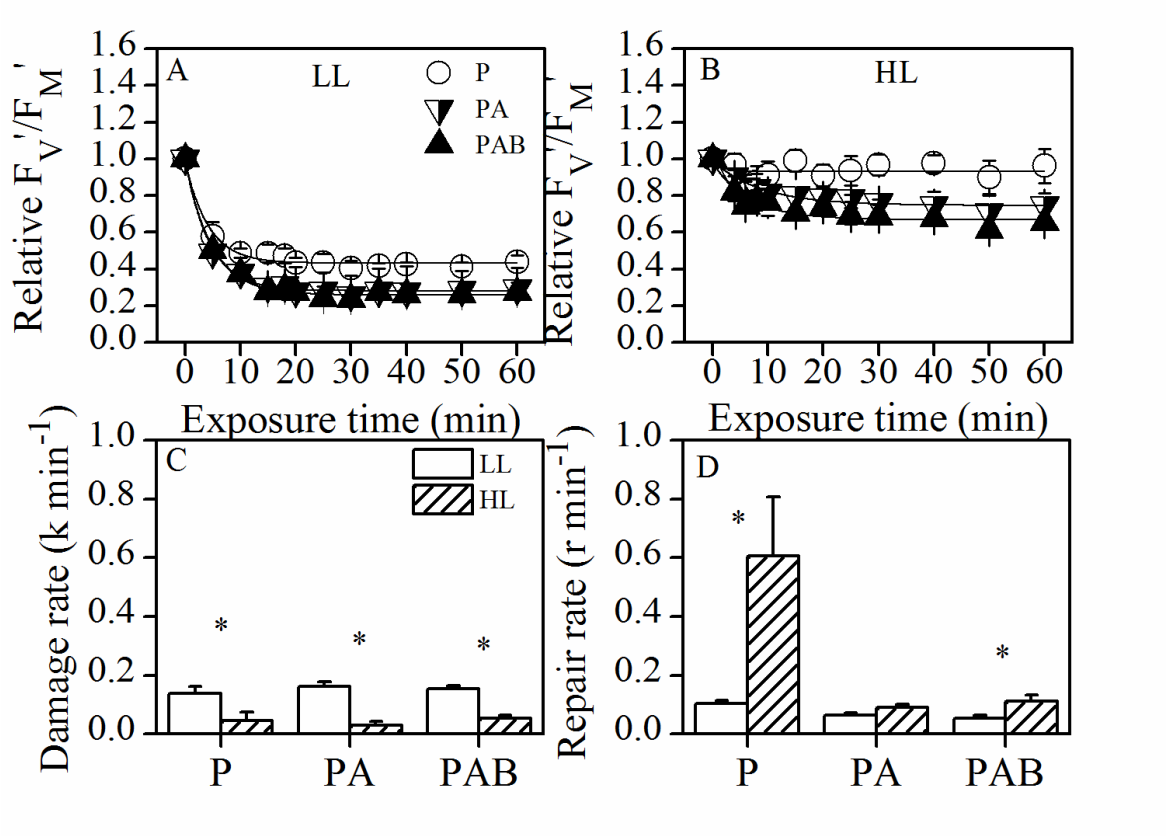

Fig.1 Changes of effective quantum yield (F_V'/F_M') of *Trichodesmium* IMS101 grown under (A) LL and (B) HL conditions while exposed to PAR (P), PAR+UVA (PA) and PAR+UVA+UVB (PAB) under solar stimulator for 60 min. PSII damage (C; k, in min^{-1}) and repair rates (D; r, in min^{-1}) of LL- and HL-grown cells were derived from the yield decline curve in the upper panels. Asterisks above the histogram bars indicate significant differences between LL- and HL-grown cells. Values are the mean ±SD, triplicate incubations.

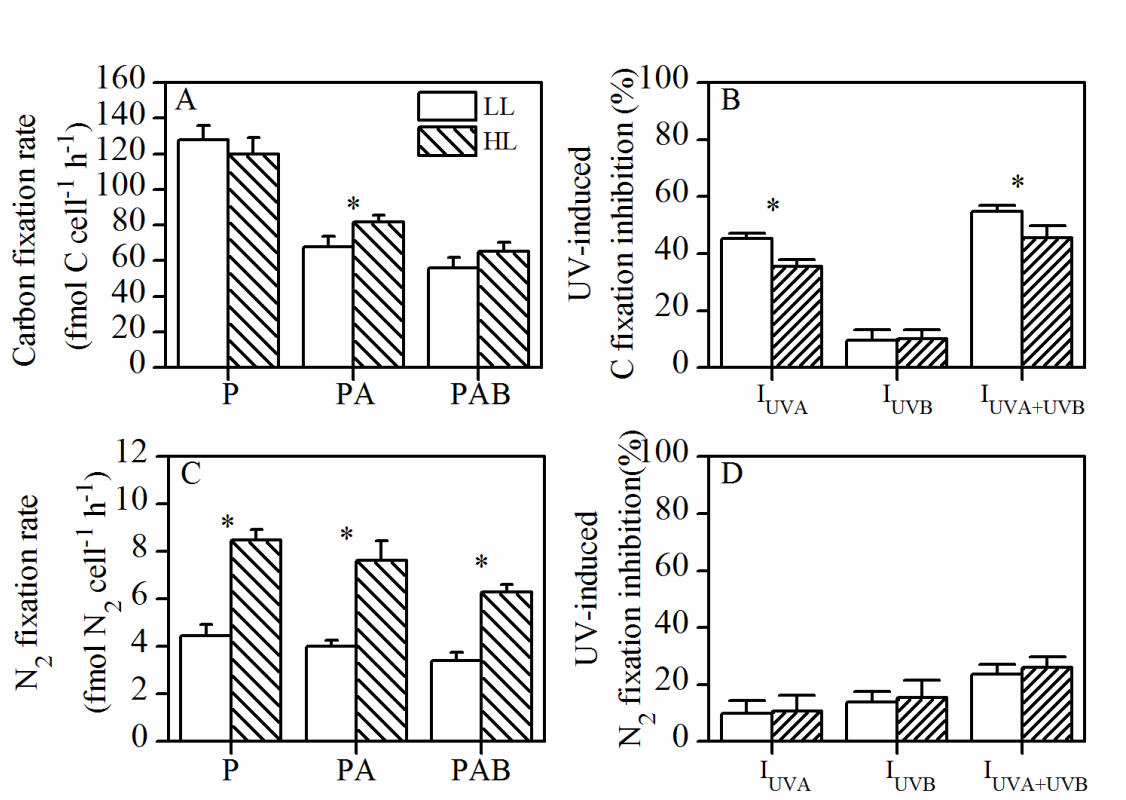

536

537 Fig.2 Photosynthetic carbon fixation rate (A; fmol C cell^{-1} h^{-1}) and UV-induced C
538 fixation inhibition (B), N_2 fixation rate (C; fmol N_2 cell^{-1} h^{-1}) and corresponding UV-
539 induced N_2 fixation inhibition (D) of *Trichodesmium* IMS101 grown under LL and HL
540 conditions. Asterisks above the histogram bars indicate significant differences between
541 LL- and HL-grown cells. Values are the mean ±SD, triplicate incubations.

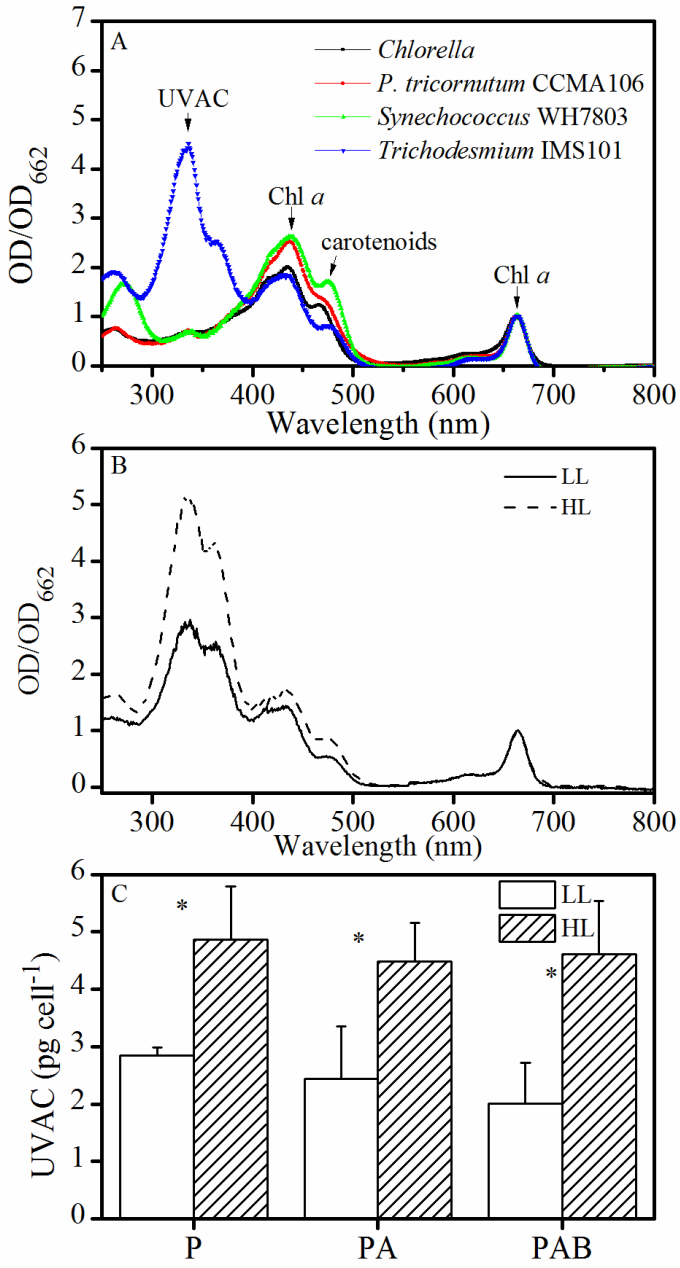

542

543 Fig.3 (A) Absorption spectrum of *Trichodesmium* IMS101 compared to other
544 phytoplankton. Pigments were extract by 100% methanol. OD value normalized to
545 OD_{662} (Chl *a*). (B) Absorption spectrum of the *Trichodesmium* IMS101 grown under
546 LL and HL conditions, OD value normalized to OD_{662} (Chl *a*). (C) Cellular contents of
547 UVACs of *Trichodesmium* IMS101 grown under LL and HL conditions after exposure
548 to PAR (P), PAR+UVA (PA), PAR+UVA+UVB (PAB) under solar stimulator for 10 h.
549 Asterisks above the histogram bars indicate significant differences between LL- and
550 HL-grown cells. Values are the mean ±SD, triplicate incubations.

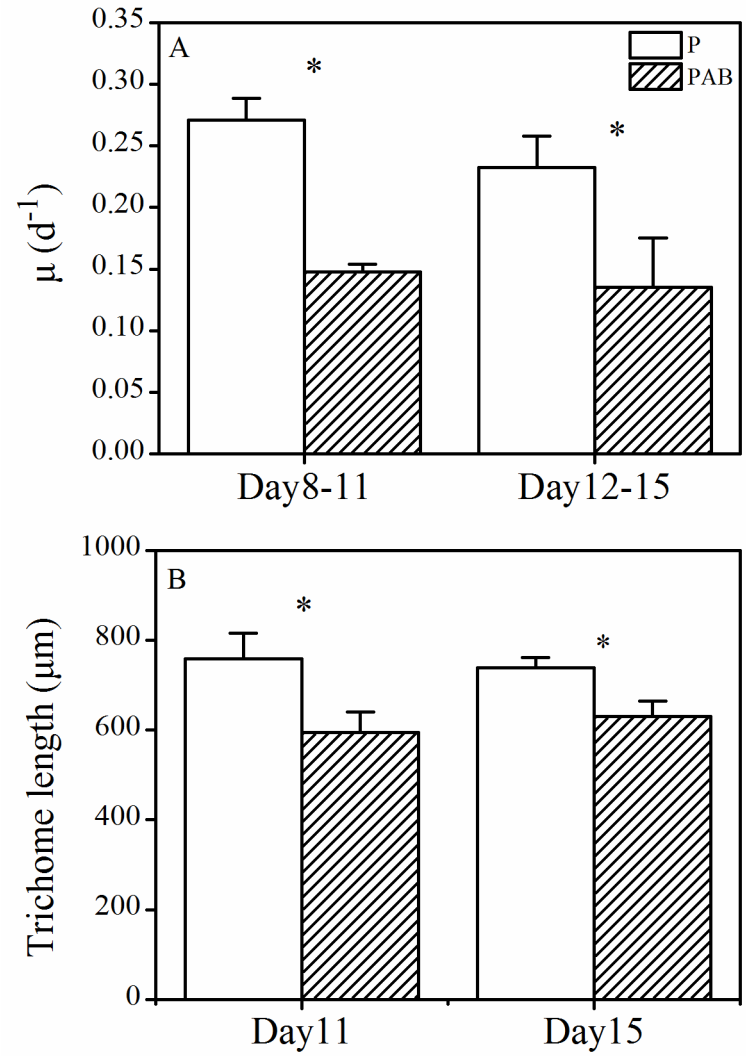

Fig.4 (A) Specific growth rate (measured during 8th-11th and 12th-15th day) of *Trichodesmium* IMS101 grown under solar PAR (P) and PAR+UVA+UVB (PAB). Corresponding total solar doses from Day 8 to Day 11 and from Day 12 to Day 15 were 17.03 and 18.51 MJ, respectively. (B) Trichome length (measured on the 11th and 15th day) of *Trichodesmium* IMS101 grown under solar PAR (P) and PAR+UVA+UVB (PAB). The asterisks indicate significant differences between radiation treatments. Values are the mean ±SD, triplicate cultures.

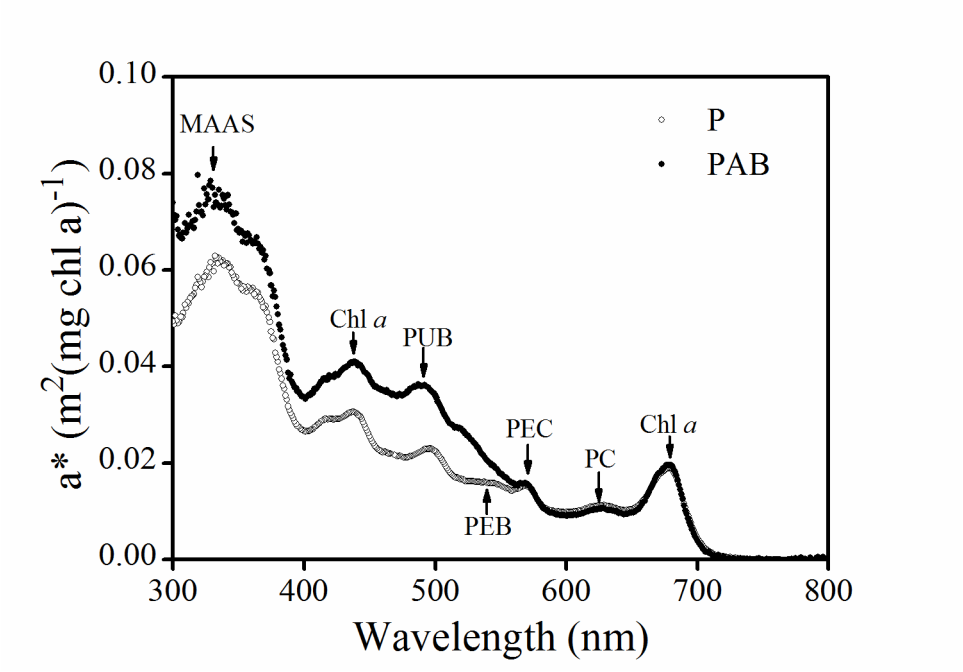

Fig.5 Chl *a* specific absorption spectrum (a^*) of *Trichodesmium* IMS101 grown under solar PAR (P) and PAR+UVA+UVB (PAB). The measurements were taken on the 18th day. The absorption peaks of MAAs (330 nm), PUB (495 nm), PEB (545 nm), PEC (569 nm), PC (625nm) and Chl *a* (438 and 664 nm) are indicated.

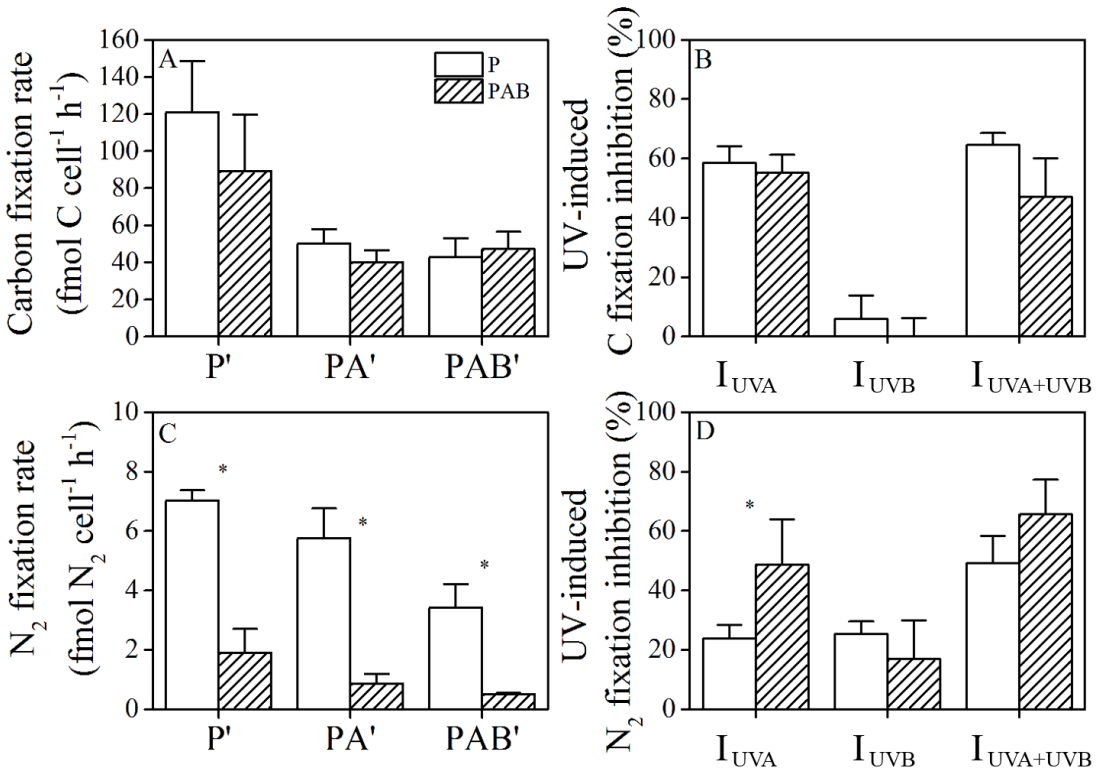

570

571 Fig. 6 Photosynthetic carbon fixation rate (A; fmol C cell^{-1} h^{-1}) and UV-induced C
572 fixation inhibition (B), N_2 fixation rate (C; fmol N_2 cell^{-1} h^{-1}) and corresponding UV-
573 induced N_2 fixation inhibition (D) of *Trichodesmium* IMS101 grown under solar PAR
574 (P) and PAR+UVA+UVB (PAB) transferred to another P′, PA′, PAB′ treatments. The
575 measurement was taken on the 18th day at 11:00~13:00. Asterisks above the histogram
576 bars indicate significant differences between P and PAB treatments. Values are the mean
577 ±SD, triplicate incubations.

578

579

580

581

582

583

584

585

586

587

588 **References**

589 1. Anning, T., Maclntyre, H. L., Sammes, S. M. P. a. P. J., Gibb, S., and Geider, R. J.:
590 Photoacclimation in the marine diatom *Skeletonema costatum*, Limnol Oceanogr,
591 1807-1817, 2000.
592 2. Bouchard, J. N., Roy, S., and Campbell, D. A.: UVB Effects on the Photosystem
593 II - D1 Protein of Phytoplankton and Natural Phytoplankton Communities,
594 Photochem Photobiol, 82, 936-951, 2006.
595 3. Breitbarth, E., Mills, M. M., Friedrichs, G., and LaRoche, J.: The Bunsen gas
596 solubility coefficient of ethylene as a function of temperature and salinity and its
597 importance for nitrogen fixation assays, Limnol. Oceanogr. Methods, 2, 282-288,
598 2004.
599 4. Cai, X., Gao, K., Fu, F., Campbell, D., Beardall, J., and Hutchins, D.: Electron
600 transport kinetics in the diazotrophic cyanobacterium *Trichodesmium* spp. grown
601 across a range of light levels, Photosyn. Res., 124, 45-56, 10.1007/s11120-015-
602 0081-5, 2015.
603 5. Campbell, D., Eriksson, M. J., Oquist, G., Gustafsson, P., and Clarke, a. K.: The
604 cyanobacterium *Synechococcus* resists UV-B by exchanging photosystem II
605 reaction-center D1 proteins., Proceedings of the National Academy of Sciences 95,
606 364-369, 1998.
607 6. Capone, D.: Determination of nitrogenase activity in aquatic samples using the
608 acetylene reduction procedure, In P. F. Kemp, B. F. Sherr, E. B. Sherr, and J. J.
609 Cole (ed.), Handbook of methods in aquatic microbial ecology. Lewis Publishers,
610 Boca Raton, Fla, p. 621–631, 1993.
611 7. Capone, D., Zehr, J., Paerl, H., and Bergman, B.: *Trichodesmium*, a globally
612 significant marine cyanobacterium, Science, 276, 1221-1227, 1997.
613 8. Capone, D. G., Subramaniaml, A., Joseph, P., Carpenters, E. J., Johansen, M., and

614 Ronald, L.: An extensive bloom of the N_2-fixing cyanobacterium *Trichodesmium*
615 *erythraeum* in the central Arabian Sea, Mar. Ecol. Prog. Ser., 172, 281-292, 1998.
616 9. Carpenter, E. J., Subramaniam, A., and Capone, D. G.: Biomass and primary
617 productivity of the cyanobacterium *Trichodesmium* spp. in the tropical N Atlantic
618 ocean, Deep Sea Research Part I: Oceanographic Research Papers, 51, 173-203,
619 10.1016/j.dsr.2003.10.006, 2004.
620 10. Chen, Y. B., Zehr, J. P., and Mellon, M.: Growth and nitrogen fixation of the
621 diazotrophic filamentous nonheterocystous cyanobacterium *Trichodesmium* sp.
622 IMS101 in defined media: evidence for a circadian rhythm, J Phycol, 32, 916-923,
623 1996.
624 11. Cleveland, J. S., and Weidemann, A. D.: Quantifying Absorption by Aquatic
625 Particles: A Multiple Scattering Correction for Glass-Fiber, Limnol Oceanogr, 38,
626 1321-1327, 1993.
627 12. Cockell, C. S., and Rothschild, L. J.: The Effects of UV Radiation A and B on
628 Diurnal Variation in Photosynthesis in Three Taxonomically and Ecologically
629 Diverse Microbial Mats, Photochem Photobiol, 69, 203-210, 10.1111/j.1751-
630 1097.1999.tb03274.x, 1999.
631 13. Cullen, J. J., and Neale, P. J.: Ultraviolet radiation, ozone depletion, and marine
632 photosynthesis, Photosyn. Res., 39, 303-320, 10.1007/bf00014589, 1994.
633 14. Dunlap, W., Rae, G., Helbling, E., Villafañe, V., and Holm-Hansen, O.: Ultraviolet-
634 absorbing compounds in natural assemblages of Antarctic phytoplankton, Antarct
635 J U S, 30, 323-326, 1995.
636 15. Fay, P.: Oxygen relations of nitrogen fixation in cyanobacteria, Microbiol. Rev., 56,
637 340-373, 1992.
638 16. Fu, F.-X., Yu, E., Garcia, N. S., Gale, J., Luo, Y., Webb, E. A., and Hutchins, D. A.:
639 Differing responses of marine N_2 fixers to warming and consequences for future
640 diazotroph community structure, Aquat. Microb. Ecol., 72, 33-46, 2014.
641 17. Garcia-Pichel, F., and W.Castenholz, R.: Occurrence of UV-

642 absorbingmycosporine-like compounds among cyanobacterial isolates and
643 estimationof their screening capacity, Appl. Environ. Microbiol., 163-169, 1993.
644 18. Genty, B., Briantais, J.-M., and Baker, N. R.: The relationship between the quantum
645 yield of photosynthetic electron transport and quenching of chlorophyll
646 fluorescence, Biochimica et Biophysica Acta (BBA) - General Subjects, 990, 87-
647 92, http://dx.doi.org/10.1016/S0304-4165(89)80016-9, 1989.
648 19. Häder, D.-P., and Gao, K.: Interactions of anthropogenic stress factors on marine
649 phytoplankton, Frontiers in Environmental Science, 3, 1-14, 2015.
650 20. Häder, D. P., Williamson, C. E., Wangberg, S. A., Rautio, M., Rose, K. C., Gao, K.,
651 Helbling, E. W., Sinha, R. P., and Worrest, R.: Effects of UV radiation on aquatic
652 ecosystems and interactions with other environmental factors, Photochem.
653 Photobiol. Sci., 14, 108-126, 10.1039/c4pp90035a, 2015.
654 21. He, Y.-Y., Klisch, M., and Häder, D.-P.: Adaptation of cyanobacteria to UV-B stress
655 correlated with oxidative stress and oxidative damage., Photochem Photobiol, 76,
656 188-196, 2002.
657 22. Heraud, P., and Beardall, J.: Changes in chlorophyll fluorescence during exposure
658 of Dunaliella tertiolecta to UV radiation indicate a dynamic interaction between
659 damage and repair processes, Photosyn. Res., 63, 123-134,
660 10.1023/a:1006319802047, 2000.
661 23. Hutchins, D. A., Walworth, N. G., Webb, E. A., Saito, M. A., Moran, D., McIlvin,
662 M. R., Gale, J., and Fu, F.-X.: Irreversibly increased nitrogen fixation in
663 *Trichodesmium* experimentally adapted to elevated carbon dioxide, Nature
664 Communication, 6, 8155, 10.1038/ncomms9155, 2015.
665 24. Karsten, U., Sawall, T., and Wiencke, C.: A survey of the distribution of UV-
666 absorbing substances in tropical macroalgae, Phycol. Res., 46, 271-279,
667 10.1046/j.1440-1835.1998.00144.x, 1998.
668 25. Kiefer, D. A., and SooHoo, J. B.: Spectral absorption by marine particles of coastal
669 waters of Baja California, Limnol Oceanogr, 27, 492-499, 1982.

26. Kranz, S. A., Levitan, O., Richter, K. U., Prasil, O., Berman-Frank, I., and Rost, B.: Combined effects of CO_2 and light on the N_2-fixing cyanobacterium *Trichodesmium* IMS101: physiological responses, Plant Physiol., 154, 334-345, 10.1104/pp.110.159145, 2010.
27. Kumar, A., Tyagi, M. B., Jha, P. N., Srinivas, G., and Singh, A.: Inactivation of cyanobacterial nitrogenase after exposure to Ultraviolet-B radiation, Curr. Microbiol., 46, 380-384, 10.1007/s00284-001-3894-8, 2003.
28. Litchman, Elena, Patrick J. Neale, and Anastazia T. Banaszak.: Increased sensitivity to ultraviolet radiation in nitrogen-limited dinoflagellates: Photoprotection and repair, Limnol Oceanogr, 47, 86-94, 2002.
29. Lesser, M. P.: Effects of ultraviolet radiation on productivity and nitrogen fixation in the Cyanobacterium, *Anabaena* sp. (Newton's strain), Hydrobiologia, 598, 1-9, 10.1007/s10750-007-9126-x, 2007.
30. Luo, Y.-W., Lima, I. D., Karl, D. M., and Doney, S. C.: Data-based assessment of environmental controls on global marine nitrogen fixation, BGeo, 11, 619-708, 2014.
31. Mitchell, B. G.: Algorithms for determining the absorption coefficient for aquatic particulates using the quantitative filter technique, Orlando'90, 16-20 April, 1990, 137-148,
32. Neale, Patrick J., Anastazia T. Banaszak, and Catherine R. Jarriel.: Ultraviolet sunscreens in *Gymnodinium sanguineum* (Dinophyceae): mycosporine-like amino acids protect against inhibition of photosynthesis. J Phycol, 34, 928-938, 1998.
33. Neale, P. J., and Thomas, B. C.: Inhibition by ultraviolet and photosynthetically available radiation lowers model estimates of depth-integrated picophytoplankton photosynthesis: global predictions for *Prochlorococcus* and *Synechococcus*, Glob Change Biol, 13356, 10.1111/gcb.13356, 2016.
34. Olson, E. M., McGillicuddy, D. J., Dyhrman, S. T., Waterbury, J. B., Davis, C. S., and Solow, A. R.: The depth-distribution of nitrogen fixation by *Trichodesmium*

698 spp. colonies in the tropical–subtropical North Atlantic, Deep Sea Research Part I:
699 Oceanographic Research Papers, 104, 72-91, 10.1016/j.dsr.2015.06.012, 2015.
700 35. Prufert-Bebout, L., Paerl, H. W., and Lassen, C.: Growth, nitrogen fixation, and
701 spectral attenuation in cultivated *Trichodesmium* species, Appl Environ Microb, 59,
702 1367-1375, 1993.
703 36. Quesada, A., Vincent, W. F., and Lean, D. R. S.: Community and pigment structure
704 of Arctic cyanobacterial assemblages: the occurrence and distribution of UV-
705 absorbing compounds, FEMS Microbiol. Ecol., 28, 315-323, 10.1111/j.1574-
706 6941.1999.tb00586.x, 1999.
707 37. Rastogi, R. P., Sinha, R. P., Moh, S. H., Lee, T. K., Kottuparambil, S., Kim, Y. J.,
708 Rhee, J. S., Choi, E. M., Brown, M. T., Hader, D. P., and Han, T.: Ultraviolet
709 radiation and cyanobacteria, J. Photochem. Photobiol. B: Biol., 141, 154-169,
710 10.1016/j.jphotobiol.2014.09.020, 2014.
711 38. Rath, J., and Adhikary, S. P.: Response of the estuarine cyanobacterium *Lyngbya*
712 *aestuarii* to UV-B radiation, J Appl Phycol, 19, 529-536, 2007.
713 39. Ritchie, R. J.: Consistent sets of spectrophotometric chlorophyll equations for
714 acetone, methanol and ethanol solvents, Photosyn. Res., 89, 27-41,
715 10.1007/s11120-006-9065-9, 2006.
716 40. Shi, D., Kranz, S. A., Kim, J. M., and Morel, F. M. M.: Ocean acidification slows
717 nitrogen fixation and growth in the dominant diazotroph *Trichodesmium* under
718 low-iron conditions, Proceedings of the National Academy of Sciences, 109,
719 E3094-E3100, 2012.
720 41. Shick, J. M., and Dunlap, W. C.: Mycosporine-like amino acids and related
721 Gadusols: biosynthesis, acumulation, and UV-protective functions in aquatic
722 organisms, Annu Rev Physiol, 64, 223-262,
723 10.1146/annurev.physiol.64.081501.155802, 2002.
724 42. Singh, Shailendra P., Sunita Kumari, Rajesh P. Rastogi, Kanchan L. Singh, and
725 Rajeshwar P. Sinha.: Mycosporine-like amino acids (MAAs): chemical structure,

biosynthesis and significance as UV-absorbing/screening compounds, Indian J Exp Biol, 46, 7-17, 2008.

43. Singh, S. P., Rastogi, R. P., Hader, D. P., and Sinha, R. P.: Temporal dynamics of ROS biogenesis under simulated solar radiation in the cyanobacterium *Anabaena variabilis* PCC 7937, Protoplasma, 251, 1223-1230, 10.1007/s00709-014-0630-3, 2014.

44. Sinha, R. P., Singh, N., Kumar, A., Kumar, H. D., Häder, M., and Häder, D. P.: Effects of UV irradiation on certain physiological and biochemical processes in cyanobacteria, J. Photochem. Photobiol. B: Biol., 32, 107-113, http://dx.doi.org/10.1016/1011-1344(95)07205-5, 1996.

45. Sinha, R. P., Singh, N., Kumar, A., Kumar, H. D., and Häder, D.-P.: Impacts of ultraviolet-B irradiation on nitrogen-fixing cyanobacteria of rice paddy fields, J Plant Physiol, 150, 188-193, http://dx.doi.org/10.1016/S0176-1617(97)80201-5, 1997.

46. Sinha, R. P., Klisch, M., Walter Helbling, E., and Häder, D.-P.: Induction of mycosporine-like amino acids (MAAs) in cyanobacteria by solar ultraviolet-B radiation, J. Photochem. Photobiol. B: Biol., 60, 129-135, http://dx.doi.org/10.1016/S1011-1344(01)00137-3, 2001.

47. Sinha, R. P., Ambasht, N. K., Sinha, J. P., Klisch, M., and Häder, D.-P.: UV-B-induced synthesis of mycosporine-like amino acids in three strains of *Nodularia* (cyanobacteria), J. Photochem. Photobiol. B: Biol., 71, 51-58, http://dx.doi.org/10.1016/j.jphotobiol.2003.07.003, 2003.

48. Sinha, R. P., and Häder, D.-P.: UV-protectants in cyanobacteria, Plant Sci., 174, 278-289, 10.1016/j.plantsci.2007.12.004, 2008.

49. Sobrino, C., and Neale, P. J.: Short-term and long-term effects of temperature on photosynthesis in the diatom *Thalassiosira Pseudonana* under UVR exposures, J Phycol, 43, 426-436, 10.1111/j.1529-8817.2007.00344.x, 2007.

50. Sohm, J. A., Webb, E. A., and Capone, D. G.: Emerging patterns of marine nitrogen

754 fixation, Nat Rev Microbiol, 9, 499-508, 10.1038/nrmicro2594, 2011.
755 51. Spungin, D., Berman-Frank, I., and Levitan, O.: *Trichodesmium*'s strategies to
756 alleviate P-limitation in the future acidified oceans, Environ. Microbiol., 16,
757 1935-1947, 10.1111/1462-2920.12424, 2014.
758 52. Subramaniam, A., Carpenter, E. J., Karentz, D., and Falkowski, P. G.: Bio-optical
759 properties of the marine diazotrophic cyanobacteria *Trichodesmium* spp. I.
760 Absorption and photosynthetic action spectra, Limnol Oceanogr, 44, 608-617,
761 1999.
762 53. Vernet, M., and Whitehead, K.: Release of ultraviolet-absorbing compounds by the
763 red-tide dinoflagellate *Lingulodinium polyedra*, Mar. Biol., 127, 35-44,
764 10.1007/bf00993641, 1996.
765 54. Villafañe, V. E., Barbieri, E. S., and Helbling, E. W.: Annual patterns of ultraviolet
766 radiation effects on temperate marine phytoplankton off Patagonia, Argentina, J
767 Plankton Res, 26, 167-174, 10.1093/plankt/fbh011, 2004.
768 55. Westberry, T. K., and Siegel, D. A.: Spatial and temporal distribution of
769 *Trichodesmium* blooms in the world's oceans, GBioC, 20, GB4016,
770 10.1029/2005gb002673, 2006.
771 56. Wu, H., Gao, K., Villafane, V. E., Watanabe, T., and Helbling, E. W.: Effects of
772 solar UV radiation on morphology and photosynthesis of filamentous
773 cyanobacterium *Arthrospira platensis*, Appl Environ Microb, 71, 5004-5013,
774 10.1128/AEM.71.9.5004-5013.2005, 2005.
775 57. Wu, H., Abasova, L., Cheregi, O., Deák, Z., Gao, K., and Vass, I.: D1 protein
776 turnover is involved in protection of Photosystem II against UV-B induced damage
777 in the cyanobacterium *Arthrospira (Spirulina) platensis*, J. Photochem. Photobiol.
778 B: Biol., 104, 320-325, http://dx.doi.org/10.1016/j.jphotobiol.2011.01.004, 2011.
779 58. Wu, Y., Li, Z., Du, W., and Gao, K.: Physiological response of marine centric
780 diatoms to ultraviolet radiation, with special reference to cell size, J. Photochem.
781 Photobiol. B: Biol., 153, 1-6, http://dx.doi.org/10.1016/j.jphotobiol.2015.08.035,

782 2015.

783